ELSEVIER

Journal of Alloys and Compounds 467 (2009) L21–L25

Journal of ALLOYS AND COMPOUNDS

www.elsevier.com/locate/jallcom

Letter

Synthesis and magnetic properties of Mg-doped hexagonal close-packed Ni nanoparticles

Jinghai Yang [a,b,*], Bo Feng [a], Yang Liu [a], Yongjun Zhang [a], Lili Yang [b,c,a], Yaxin Wang [a], Maobin Wei [a], Jihui Lang [a], Dandan Wang [a]

[a] *The Institute of Condensed State Physics, Jilin Normal University, Siping 136000, People's Republic of China*
[b] *Key Laboratory of Excited State Processes, Changchun Institute of Optics, Fine Mechanics and Physics, Chinese Academy of Sciences, Changchun 130033, People's Republic of China*
[c] *Graduate School of the Chinese Academy of Sciences, Beijing 100049, People's Republic of China*

Received 22 November 2007; received in revised form 16 December 2007; accepted 19 December 2007
Available online 28 December 2007

Abstract

Mg-doped Ni nanoparticles with the hexagonal close-packed (hcp) and face-centered cubic (fcc) structure have been synthesized by sol–gel method sintered at different temperatures in argon atmosphere. The structure, morphology and magnetic properties of the samples were studied by X-ray diffraction, TEM, VSM magnetometers and Magnetic Property Measurement System (Quantum Design MPMS XL-7), respectively. X-ray diffraction and TEM results showed that Ni–Mg solid solution was formed with the single phase of hexagonal close-packed structure. When the temperature reached 450 °C, a temperature-induced phase transform from hcp to fcc was observed. The average particle size of the sample with hcp structure evaluated by Scherrer equation was about 6.0 nm. Moreover, the VSM results demonstrated the existence of ferromagnetic behavior in both synthesized hcp and fcc Mg-doped Ni nanoparticles. The saturation magnetization (M_s) of all the samples was below that of bulk Ni (54 emu/g). Nevertheless, the magnetic measurement at 5000 Oe field for the sample with hcp structure showed that the unsaturated magnetization in hcp Mg-doped Ni nanoparticles was much smaller than that of the fcc Mg-doped Ni nanoparticles. From the *M–T* curves, the blocking temperature (T_B) of the hcp Mg-doped Ni nanoparticles was estimated to be 10 K. It was also found that changes of the stress, particle size and structure during heat-treating had significant influences on the magnetic properties of the Mg-doped Ni nanoparticles.

Keywords: Nanostructured materials; Sol–gel processes; Phase transitions; Magnetization

1. Introduction

In recent years, nanoparticles of ferromagnetic metals such as Fe, Co and Ni attract more and more interests in terms of their special physical properties and potential applications in catalysts, high density magnetic recording media, medical diagnostics, ferrofluids, and biomedical fields [1–5]. Among these ferromagnetic metals, Ni nanoparticles were investigated owing to their potential application in magnetic sensors and memory devices [6–9]. Different methods were used to prepare Ni nanoparticles and their magnetic properties were also investigated. According to these reports, face-centered cubic (fcc) structure was its equilibrium bulk phase. Another polymorph, the hexagonal close-packed (hcp) structure, was a metastable phase observed mainly in thin films under specific conditions [10,11]. Therefore, most samples prepared with different chemical methods existed with the face-centered cubic structure. In other words, only a little work has been reported on the free-standing hcp nickel because of the difficulties in synthesis. Chinnasamy et al. obtained a mixture of fcc and hcp Ni nanoparticles with dimensions of tens of nanometers by the reduction in trimethylene glycol under alkaline condition [12]. Carturan et al. prepared hcp Ni powder by nickel acetyl acetonate reacting with K/B alloy in an inert atmosphere [13]. Mi et al. obtain hexagonal close-packed nanocrystalline nickel by a thermal reduction process [14]. However, there were contradicting theoretical reports on the magnetic properties of the hcp Ni nanoparticles [15].

* Corresponding author at: The Institute of Condensed State Physics, Jilin Normal University, Siping 136000, People's Republic of China.
Tel.: +86 434 3290009; fax: +86 434 3294566.
E-mail address: jhyang1@jlnu.edu.cn (Jinghai Yang).

0925-8388/$ – see front matter © 2008 Elsevier B.V. All rights reserved.
doi:10.1016/j.jallcom.2007.12.068

In this work, the simple and easy sol–gel method is used to obtain high-quality metal and alloy powders of controlled structure, morphology, size and size distribution. Some researchers report that additions of alloying elements have been shown to improve the thermal stability of the material with hcp structure. There are only few detailed reports on the preparation of hcp Mg-doped Ni nanoparticles using sol–gel method [16]. To make the hexagonal close-packed structure more stable, and to understand the magnetic mechanism of the metastable phase for ferromagnetic metals, we decide to synthesize Mg-doped Ni nanoparticles because the equilibrium bulk phase of unalloyed Mg has a hexagonal close-packed structure. The phase transition and magnetic properties are also studied.

2. Experimental details

All chemical reagents in this work were of analytical grade purity. The initial materials included Ni $(NO_3)_2{\cdot}6H_2O$, $Mg(NO_3)_2{\cdot}6H_2O$ and citrate ($C_6H_8O_7{\cdot}H_2O$). The appropriate stoichiometric proportions of Ni $(NO_3)_2{\cdot}6H_2O$, $Mg(NO_3)_2{\cdot}6H_2O$ and citrate ($C_6H_8O_7{\cdot}H_2O$) were weighed (Ni:Mg = 0.95:0.05, in mol) and their solution were mixed. The mixture had been homogenized with stirring for 2 h to form a sol and subsequently polymerized to form a gel at 80 °C. The gel was prepyrolyzed to become an amorphous composite precursor at 120 °C. At a final step, the Mg-doped Ni nanoparticles were successfully synthesized with precursors heat-treated in argon gases for 10 h at different temperatures of 320, 350 and 450 °C, respectively. The process is:

$$C_6H_8O_7{\cdot}H_2O + Ni(NO_3)_2{\cdot}6H_2O + Mg(NO_3)_2{\cdot}6H_2O \rightarrow CO + NO_2 + H_2O + Ni\text{–}Mg$$

Both hydroxyl of the citrate and the carbon monoxide with reducing power which is given off during the process of sintering the precursors will stop oxygenization of nanoparticles [17].

Structural characterization was performed by XRD on D/max-2500 copper rotating-anode X-ray diffractometer by using Cu Kα radiation (40 kV, 200 mA). Transmission electron microscope (TEM) (200 keV, JEM-2100HR, Japan) was used to investigate the morphology. The magnetic properties of the samples were measured at room temperature by a Lake Shore 7407 vibrating sample magnetometer. Magnetization versus temperature was obtained by using Magnetic Property Measurement System (Quantum Design MPMS XL-7).

3. Results and discussion

3.1. XRD characterization

The XRD of the sample synthesized at 320 °C shows the diffractions from the (0 1 0), (0 0 2), (0 1 1), (0 1 2), (1 1 0), (1 0 3), (1 1 2) and (2 0 0) planes of hcp Ni, indicating that the homogenous solid solution formation with the space group $P6_3/mmc$ and the cell constant is estimated to be $a = 2.6514 \pm 0.0003$ Å, $c = 4.3436 \pm 0.0007$ Å, and the volume is 0.0264 nm^3 (Fig. 1a). Particle size obtained by Scherrer formula is 6.0 nm.

Fig. 1b and c shows the XRD patterns of the samples synthesized at 350 and 450 °C. When the heat-treating temperature goes on increasing to 350 °C (Fig. 1b), the diffraction peaks at $2\theta = 44.6°$, 51.8° and 76.3° that are attributable to fcc Ni (1 1 1), (2 0 0) and (2 2 0) appear, this indicates that the samples are mixed by hcp and fcc Ni in the samples. When the heat-treating temperature increases to 450 °C (Fig. 1c), the intensity of fcc Ni (1 1 1) peak increases significantly and only one fcc Ni phase is found at this temperature. With the growth of temperature, the appearance of fcc Ni phase shows that the hcp structure of Ni is metastable. The temperature of phase transformation is between 350 and 450 °C and this temperature is higher than the phase transformation temperature of Ni [17]. The average particle size of the fcc Mg-doped Ni nanoparticles is calculated to be 10 nm by Scherrer equation. The cell constant is estimated to be $a = 3.5211 \pm 0.0003$ Å and the volume of lattice (V_0) is 0.0437 nm^3, which is smaller than that of Ni, this indicates that Mg is doped in Ni [13]. One of the possible explanations for the decreases of the cell constant is that some vacancies will occur in crystal lattice due to Mg doping, thus the cell constant will decrease with the increase of the number of the lattice which the vacancy has occupied. Moreover, the Gibbs–Thomson equation is $\Delta C^B(T, D) = 4\Omega\gamma C_0^B / KTD$ [18], where $\Delta C^B(T, D)$ is the variation of density of solid solubility, Ω is the volume of an atom, γ is the surface energy, C_0^B is the equilibrium solid solubility, D is the particle size, and K is the Boltzman constant. So the smaller the particle size becomes and the more the solid solubility increases, the more lattice will be occupied by vacancies, and at the same time, the cell constant will become smaller, in other words, the contraction of the volume of the cell will become more. However, accurate identification of such a lattice contraction needs further studies.

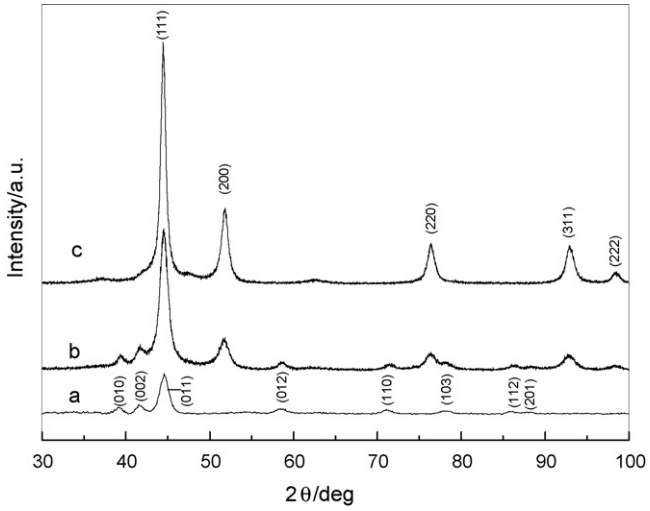

Fig. 1. XRD patterns for the samples synthesized at 320 °C (a), 350 °C (b) and 450 °C (c).

3.2. TEM characterization

Fig. 2 shows the TEM image of the samples synthesized at 320 and 450 °C. The observation shows the nanostructured alloy of spherical shape and narrow size distribution. The average particle size is about 6.0 nm for a, and about 10 nm for b, in agreement with the results of the XRD.

3.3. Magnetic properties

Fig. 3 shows the hysteresis loops of hcp Mg-doped Ni nanoparticles measured at room temperature. The hcp Mg-doped Ni nanoparticles have a coercivity of 32.906 Oe and are not sat-

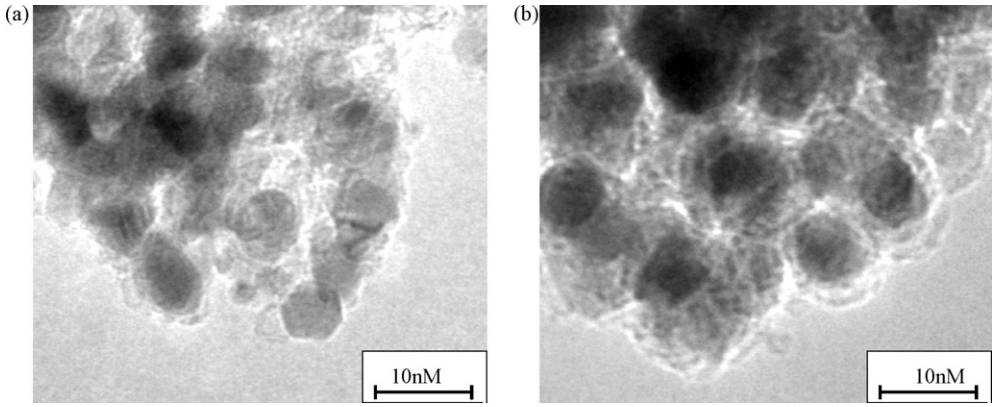

Fig. 2. TEM image of samples synthesized at 320 °C (a) and 450 °C (b).

urated in the maximum field of 5000 Oe. The room-temperature magnetic properties can be understood in terms of the particle size distribution, independent of the synthetic process. Because of the particle size distribution of the samples, the samples have ferromagnetic behavior when the particle size is bigger than the superparamagnetic critical size, while superparamagnetic behavior when smaller than it. In our opinion, the hcp Mg-doped Ni nanoparticles have ferromagnetic behavior. This ferromagnetic behavior is in accordance with the theory of Papa et al. [19] and is similar to Mi et al. [14], but differs from magnetic behavior of Ni nanoparticles reported by Jeon et al. [20]. Mi et al. reported that the hysteresis loop of the hcp Ni obtained by a thermal reduction process indicated a ferromagnetic behavior with saturation magnetization of 7.4 emu/g and coercivity values of 94 Oe [14]. However, Jeon et al. reported that the hcp Ni particles of 8.5–18 nm sizes should be antiferromagnetic or paramagnetic, with the H_c values of zero [20]. It turns out to be the fact that the hcp Mg-doped Ni nanoparticles have unique ferromagnetic and superparamagnetic behavior.

Fig. 4 shows the hysteresis loops of the samples prepared at 350 and 450 °C when they are measured at room temperature. The higher annealing temperature led to the phase transition from hcp to fcc structure gradually. Annealing at 350 °C led to the mixture of soft magnetic hcp phase and ferromagnetic fcc phase (Fig. 4), and the saturation magnetization and the coercivity were 23.223 emu/g and 18.8595 Oe, respectively. When the annealing temperature increased to 450 °C, the transition from hcp structure to fcc structure was completed and the resultant sample was ferromagnetic Mg-doped Ni nanoparticles with

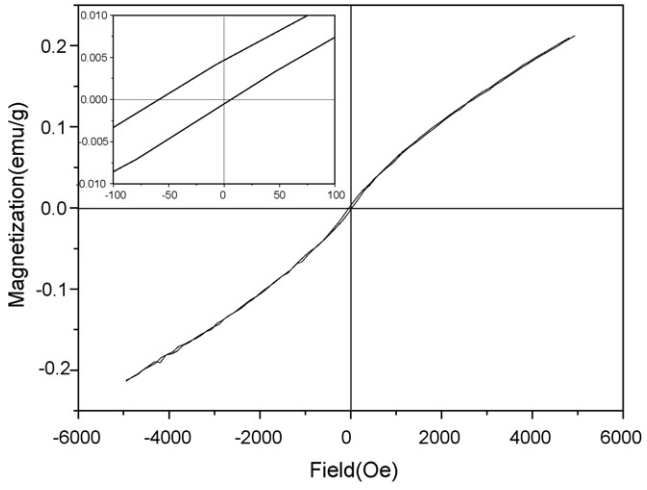

Fig. 3. Hysteresis loops of hcp Mg-doped Ni nanoparticles measured at room temperature.

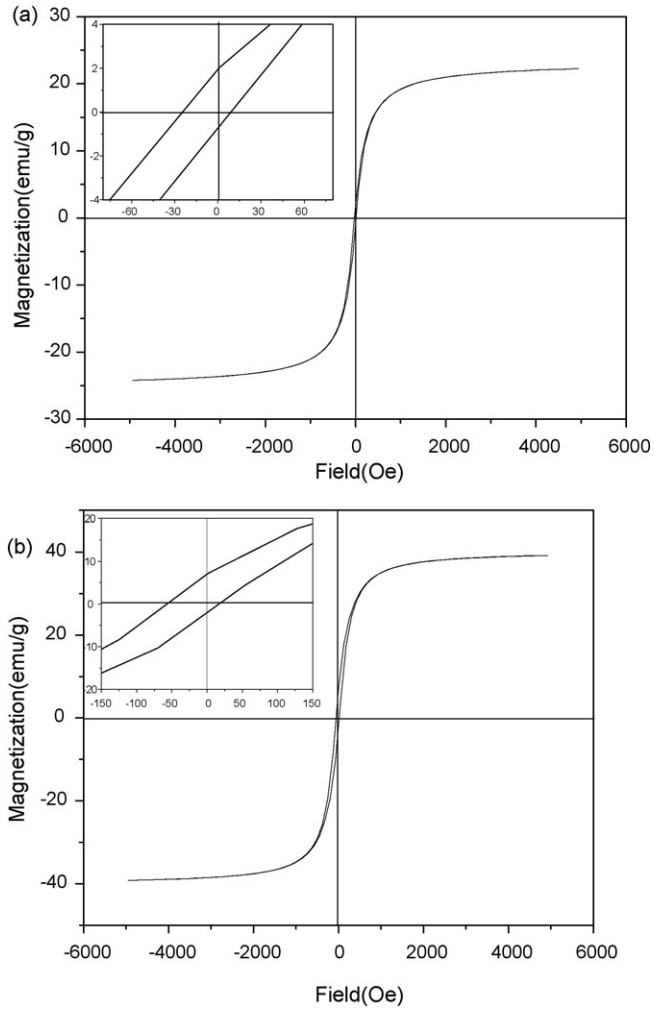

Fig. 4. Hysteresis loops of samples obtained at 350 °C (a) and 450 °C (b).

Table 1
The coercivity and M_s of the samples synthesized at different temperatures

Samples	(a) 320 °C	(c) 350 °C	(d) 450 °C
Structure	hcp	hcp/fcc	fcc
Particle size (nm)	6.0	7.3/7.7	10
Coercivity (Oe)	32.906	18.860	37.103
M_s (emu/g)		23.223	39.232

fcc structure, as is shown in Fig. 4b, and the saturation magnetization and the coercivity were 39.232 emu/g and 37.103 Oe, respectively. The evolutions of coercivity and M_s are listed in Table 1. The abnormal decrease of coercivity annealed at 350 °C may be explained by the coexistence of two phases, magnetic interaction and crystal lattice defect.

The temperature-dependent magnetization (M–T) of the Mg-doped Ni nanoparticles was also measured under zero-field-cooled (ZFC) and 100 Oe field-cooled (FC) conditions (Fig. 5). For the hcp Mg-doped Ni nanoparticles (Fig. 5a), the ZFC curve agrees with FC curve very well along the high temperature side, and the deviation happens below 25 K. A sharp peak corresponding to the blocking temperature (T_B) of the hcp Mg-doped Ni nanoparticles is observed at around 10 K. The observed

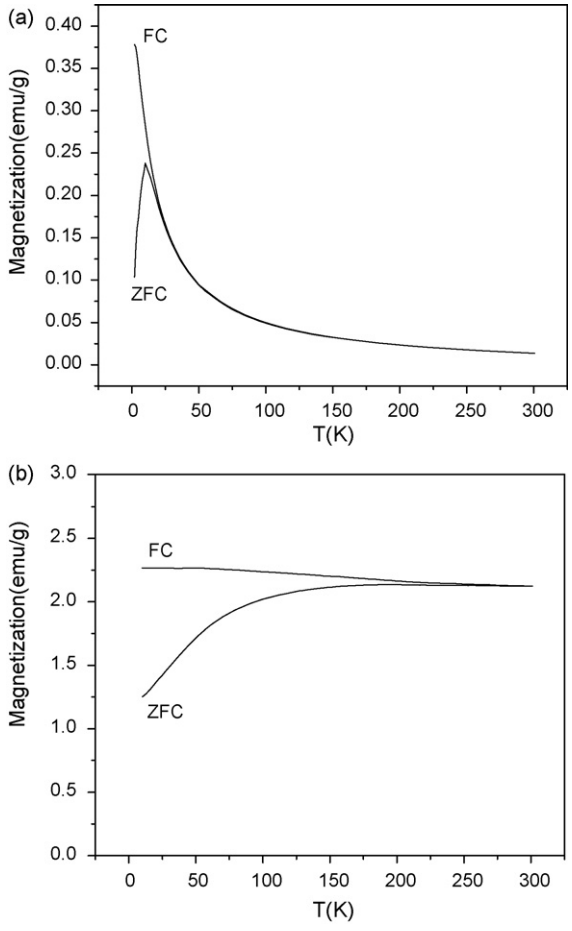

Fig. 5. Zero-field-cooled (ZFC) and field-cooled (FC) magnetization versus temperature curves for hcp Mg-doped Ni nanoparticles (a) and fcc Mg-doped Ni nanoparticles (b).

behavior reveals the progressive blocking of the superparamagnetic particle moments, with a distribution of relaxation time to the size and anisotropy axis direction. A small dependence of T_B values on the particle size is observed [20]. That is T_B generally increases with increasing particle size, and the T_B value of 10 K is smaller than that of 12 K (13.2 nm) and 12.5 K (25 nm) [21]. In the FC curve, the magnetization continues to increase below the peak temperature T_B without a tendency towards saturation, this shows superparamagnetic particles in the hcp Mg-doped Ni nanoparticles, not spin-glass or spin-canting [22]. It leads to the result that the temperature dependence of the low-field magnetization depends on the type of anisotropy energy barrier for an assembly of non-interacting magnetic nanoparticles.

However, the ZFC-FC magnetization curves of the fcc Mg-doped Ni nanoparticles are quite different from those of the hcp Mg-doped Ni nanoparticles. For the fcc Mg-doped Ni nanoparticles (Fig. 5b), the ZFC magnetization monotonically increases with increasing temperature and the FC magnetization decreases. The T_B value of the fcc Mg-doped Ni nanoparticles is estimated to be 195 K. Compared to those fcc nickel nanoparticles with bigger sizes [9,20], the as-synthesized fcc Mg-doped Ni nanoparticles with average size of 10 nm possess a lower blocking temperature. Also this can be attributed to the size-dependent properties of blocking temperature.

Fig. 6 shows the hysteresis (M–H) curves of the hcp Mg-doped Ni nanoparticles measured at 5 K. The magnetization is reversible without saturation even for 5000 Oe magnetic field, which suggests the existence of two contributions: $M = M_{irr} + M_{rev}$. M_{irr} corresponds to the blocked regime of the component responsible for the Langevin behavior at high temperature (M_s), whereas M_{rev} is related to the liner component (χ_H) [23].

Jeon et al. proposed that the hcp Ni nanoparticles seemed to be antiferromagnetic for $T > T_B$ and similar results were reported by some other researchers [20,23,24], implying that the hcp Ni nanoparticles can also be nonmagnetic or antiferromagnetic. But these conclusions are not supported by our experiments. We

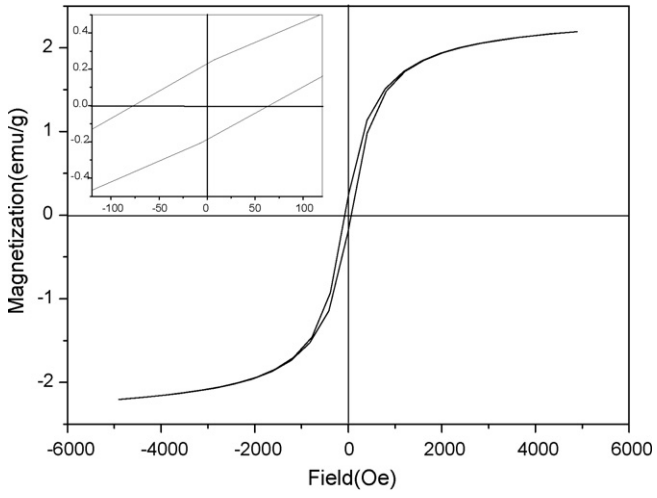

Fig. 6. Hysteresis loops of hcp Mg-doped Ni nanoparticles measured at 5 K.

think that the hcp Mg-doped Ni nanoparticles are ferromagnetic. The ZFC and FC curves show that magnetic properties of the hcp Mg-doped Ni nanoparticles within superparamagnetic critical dimension.

4. Conclusion

The synthesis of Mg-doped Ni nanoparticles with hexagonal close-packed and face-centered cubic structure by sol–gel method was reported. X-ray diffraction and TEM results showed that Ni–Mg solid solution was formed. When the temperature increased to 450 °C, a temperature-induced phase transformation from hcp to fcc was observed. And the magnetic properties of the samples were studied by recording both the temperature-dependent magnetization (*M–T*) and hysteresis (*M–H*) curves. The results demonstrated the existence of ferromagnetic behavior in both hcp and fcc Mg-doped Ni nanoparticles. Moreover, the magnetic state of hcp Mg-doped Ni nanoparticles was different from that of the fcc Mg-doped Ni nanoparticles. The ZFC magnetization curve presented T_B ($\approx$10 K) for the hcp Mg-doped Ni nanoparticles and T_B ($\approx$195 K) for the fcc Mg-doped Ni nanoparticles.

Acknowledgements

This work is supported by the National Natural Science Foundation of China (Grant Nos. 60778040), gifted youth program of Jilin province (No. 20060123) and the science and technology bureau of Key Program for Ministry of Education (Item No. 207025).

References

[1] L. Schultz, K. Schnitzke, J. Wecker, Appl. Phys. Lett. 56 (1990) 868.
[2] L. Lu, M.L. Sui, K. Lu, Science 287 (2000) 1463.
[3] H. Gleiter, Nanostruct. Mater. 1 (1992) 1.
[4] M.-P. Pileni, Adv. Funct. Mater. 11 (2001) 323.
[5] S. Sun, C.B. Murray, D. Weller, L. Folks, A. Moser, Science 287 (2000) 1989.
[6] Z.K. Wang, M.H. Kuok, S.C. Ng, D.J. Lockwood, M.G. Cottam, K. Nielsch, R.B. Wehrpohn, U. Gosele, Phys. Rev. B 87 (2002) 27201.
[7] K.B. Lee, S. Park, C.A. Mirkin, Angew. Chem. Int. Ed. 43 (2004) 3048.
[8] C. Beeli, Nanostruct. Mater. 11 (1999) 697.
[9] Y. Chen, D.L. Peng, D. Lin, X. Luo, Nanotechnology 18 (2007) 505703.
[10] J. Tuaillon, V. Dupuis, P. Melinon, B. Prevel, M. Treilleux, A. Perez, M. Pellarin, J.L. Vialle, M. Broyer, Philos. Mag. A 76 (1997) 493.
[11] Y. Mi, D. Yuan, Y. Liu, J. Zhang, Y. Xiao, Mater. Chem. Phys. 89 (2005) 359.
[12] C.N. Chinnasamy, B. Jeyadevan, K. Shinoda, K. Tohji, A. Narayanasamy, K. Sato, S. Hisano, J. Appl. Phys. 97 (10) (2005) J309.
[13] G. Carturan, G. Cocco, S. Enzo, R. Ganzerla, M. Lenarda, Mater. Lett. 7 (1988) 47.
[14] Y.Z. Mi, D.S. Yuana, Y.L. Liu, et al., Mater. Chem. Phys. 89 (2005) 359.
[15] D.A. Papaconstantopoulos, J.L. Fry, N.E. Brener, Phys. Rev. B 39 (1989) 2526.
[16] K.-J. Jeon, et al., Int. J. Hydrogen Energy 32 (2007) 1860.
[17] J. Gong, Y. Liu, L.-L. Wang, et al., Chem. Res. Chin. U. 28 (2007) 1232.
[18] P.G. Shewmon, Transformation in Materials, McGraw-Hill, New York, 1969, p. 3004.
[19] D.A. Papa, J.L. Fry, N.E. Brener, Phys. Rev. B 39 (1989) 2526.
[20] Y.T. Jeon, J.Y. Moon, G.H. Lee, et al., J. Phys. Chem. B 110 (2006) 1187.
[21] V. Tzitzios, G. Basina, M. Gjoka, et al., Nanotechnology 17 (2006) 3750.
[22] T. Bitoh, K. Ohba, M. Takamatsu, T. Shirane, S. Chikazawa, J. Phys. Soc. 64 (1995) 1305.
[23] J. Vergara, V.J. Madurga, Mater. Res. 17 (2002) 2099.
[24] S.M. Zharkov, V.S. Zhigalov, G.I. Frolov, Phys. Met. Metall. 81 (1996) 170.